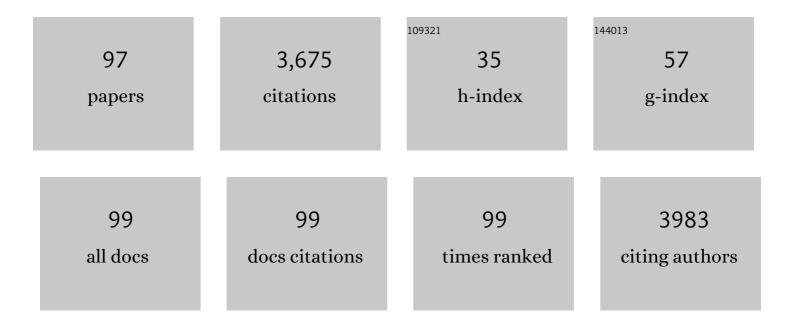
List of Publications by Year in descending order

Source: https://exaly.com/author-pdf/1096568/publications.pdf Version: 2024-02-01



IINAWEN SHI

#	Article	IF	CITATIONS
1	Rapid high-temperature hydrothermal post treatment on graphitic carbon nitride for enhanced photocatalytic H2 evolution. Catalysis Today, 2023, 409, 94-102.	4.4	54
2	Regulation on polymerization degree and surface feature in graphitic carbon nitride towards efficient photocatalytic H2 evolution under visible-light irradiation. Journal of Materials Science and Technology, 2022, 98, 160-168.	10.7	45
3	Photocatalytic overall water splitting without noble-metal: Decorating CoP on Al-doped SrTiO3. Journal of Colloid and Interface Science, 2022, 606, 491-499.	9.4	27
4	Significantly enhanced photothermal catalytic hydrogen evolution over Cu2O-rGO/TiO2 composite with full spectrum solar light. Journal of Colloid and Interface Science, 2022, 608, 2058-2065.	9.4	53
5	Accelerating the search of CHONF-containing highly energetic materials by combinatorial library design and high-throughput screening. Fuel, 2022, 310, 122241.	6.4	15
6	Architecture latticeâ€matched cauliflowerâ€like <scp>CuO</scp> / <scp>ZnO</scp> p–n heterojunction toward efficient water splitting. Journal of Chemical Technology and Biotechnology, 2022, 97, 914-923.	3.2	4
7	Numerical simulation on natural convection and temperature distribution of supercritical water in a side-wall heated cavity. Journal of Supercritical Fluids, 2022, 181, 105465.	3.2	21
8	Synergistic effect of nitrogen vacancy on ultrathin graphitic carbon nitride porous nanosheets for highly efficient photocatalytic H2 evolution. Chemical Engineering Journal, 2022, 431, 134101.	12.7	74
9	Experimental investigation on the production of hydrogen from discarded circuit boards in supercritical water. International Journal of Hydrogen Energy, 2022, 47, 31773-31785.	7.1	4
10	Morphologies dependence of hydrogen evolution over CeO2 via ultrasonic triggering. International Journal of Hydrogen Energy, 2022, 47, 15149-15159.	7.1	9
11	Study on Carbon Fixation and Gasification of Polypropylene and Polycarbonate in a CO <sub>2</sub> Environment. Industrial & Engineering Chemistry Research, 2022, 61, 10436-10445.	3.7	6
12	Study on supercritical water gasification reaction and kinetic of coal model compounds. Fuel Processing Technology, 2022, 230, 107210.	7.2	10
13	EDTA-dominated hollow tube-like porous graphitic carbon nitride towards enhanced photocatalytic hydrogen evolution. Journal of Colloid and Interface Science, 2022, 619, 289-297.	9.4	14
14	Photoelectrochemical oxygen evolution with interdigitated array electrodes: the example of TiO <sub>2</sub> . Nanotechnology, 2022, 33, 325701.	2.6	2
15	Shear-Induced Aggregation and Distribution in Photocatalysis Suspension System for Hydrogen Production. Industrial & Engineering Chemistry Research, 2022, 61, 6722-6732.	3.7	2
16	Transferring the available fused cyclic scaffolds for high—throughput combinatorial design of highly energetic materials via database mining. Fuel, 2022, 324, 124591.	6.4	14
17	Photo-inactive ZIF-8 is applied to significantly enhance the photocatalytic water reduction by forming a built-in electric field with g-C3N4 and the mechanism analysis. Journal of Environmental Chemical Engineering, 2022, 10, 107998.	6.7	4
18	Facile oneâ€pot pyrolysis preparation of <scp>SnO<sub>2</sub></scp> / <scp>gâ€C<sub>3</sub>N<sub>4</sub></scp> composites for improved photocatalytic <scp>H<sub>2</sub></scp> production. Journal of Chemical Technology and Biotechnology, 2022, 97, 2921-2931.	3.2	2

#	Article	IF	CITATIONS
19	(Oxy)nitride heterojunction-strengthened separation of photogenerated carriers in g-C3N4 towards enhanced photocatalytic H2 evolution. Applied Catalysis A: General, 2022, 643, 118746.	4.3	13
20	MoO3/g-C3N4 Z-scheme (S-scheme) system derived from MoS2/melamine dual precursors for enhanced photocatalytic H2 evolution driven by visible light. International Journal of Hydrogen Energy, 2021, 46, 2927-2935.	7.1	59
21	A molecular dynamics simulation study on solubility behaviors of polycyclic aromatic hydrocarbons in supercritical water/hydrogen environment. International Journal of Hydrogen Energy, 2021, 46, 2899-2904.	7.1	55
22	Eosin Y bidentately bridged on UiO-66-NH2 by solvothermal treatment towards enhanced visible-light-driven photocatalytic H2 production. Applied Catalysis B: Environmental, 2021, 280, 119385.	20.2	92
23	NiCo <sub>2</sub> O <sub>4</sub> nanosheets as a novel oxygen-evolution-reaction cocatalyst <i>in situ</i> bonded on the g-C <sub>3</sub> N <sub>4</sub> photocatalyst for excellent overall water splitting. Journal of Materials Chemistry A, 2021, 9, 12299-12306.	10.3	92
24	Hydrogen Production from Supercritical Water Gasification of Lignin and Cellulose with Coprecipitated CuO–ZnO and Fe <sub>2</sub> 0 <sub>3</sub> –Cr <sub>2</sub> O <sub>3</sub> . Industrial & Engineering Chemistry Research, 2021, 60, 7033-7042.	3.7	17
25	High AC and DC Electroconductivity of Scalable and Economic Graphite–Diamond Polylactide Nanocomposites. Materials, 2021, 14, 2835.	2.9	6
26	Unconventional High-Index Facet of Iridium Boosts Oxygen Evolution Reaction: How the Facet Matters. ACS Catalysis, 2021, 11, 8239-8246.	11.2	23
27	Biochar production by coconut shell gasification in supercritical water and evolution of its porous structure. Journal of Analytical and Applied Pyrolysis, 2021, 156, 105151.	5.5	30
28	Nanosized BaSnO <sub>3</sub> as Electron Transport Promoter Coupled with g <sub>3</sub> N <sub>4</sub> toward Enhanced Photocatalytic H <sub>2</sub> Production. Advanced Sustainable Systems, 2021, 5, 2100138.	5.3	13
29	<scp>Intraâ€Ring</scp> Bridging: A Strategy for Molecular Design of Highly Energetic Nitramines. Chinese Journal of Chemistry, 2021, 39, 2857-2864.	4.9	6
30	Disordered nitrogen-defect-rich porous carbon nitride photocatalyst for highly efficient H2 evolution under visible-light irradiation. Carbon, 2021, 181, 193-203.	10.3	81
31	Strain effect on oxygen evolution reaction of the SrTiO3 (0 0 1) surface. Applied Physics Letters, 2021, 119, .	3.3	4
32	Recent progress on sorption/desorption-based atmospheric water harvesting powered by solar energy. Solar Energy Materials and Solar Cells, 2021, 230, 111233.	6.2	45
33	Recent progress of energy harvesting and conversion coupled with atmospheric water gathering. Energy Conversion and Management, 2021, 246, 114668.	9.2	29
34	Facile layer-by-layer self-assembly of 2D perovskite niobate and layered double hydroxide nanosheets for enhanced photocatalytic oxygen generation. International Journal of Hydrogen Energy, 2021, 46, 34276-34286.	7.1	10
35	Bridging regulation in graphitic carbon nitride for band-structure modulation and directional charge transfer towards efficient H2 evolution under visible-light irradiation. Journal of Colloid and Interface Science, 2021, 601, 220-228.	9.4	19
36	Accelerating Molecular Design of Cage Energetic Materials with Zero Oxygen Balance through Large-Scale Database Search. Journal of Physical Chemistry Letters, 2021, 12, 11591-11597.	4.6	23

#	Article	IF	CITATIONS
37	Layered perovskite oxides and their derivative nanosheets adopting different modification strategies towards better photocatalytic performance of water splitting. Renewable and Sustainable Energy Reviews, 2020, 119, 109527.	16.4	64
38	Facile preparation of nanosized MoP as cocatalyst coupled with g-C3N4 by surface bonding state for enhanced photocatalytic hydrogen production. Applied Catalysis B: Environmental, 2020, 265, 118620.	20.2	153
39	One-pot fabrication of 2D/2D HCa <sub>2</sub> Nb <sub>3</sub> O <sub>10</sub> /g-C <sub>3</sub> N <sub>4</sub> type II heterojunctions towards enhanced photocatalytic H <sub>2</sub> evolution under visible-light irradiation. Catalysis Science and Technology. 2020. 10. 5896-5902.	4.1	15
40	Surface Recombination Passivation of the BiVO <sub>4</sub> Photoanode by the Synergistic Effect of the Cobalt/Nickel Sulfide Cocatalyst. ACS Applied Energy Materials, 2020, 3, 9089-9097.	5.1	26
41	Synchronous construction of CoS2 in-situ loading and S doping for g-C3N4: Enhanced photocatalytic H2-evolution activity and mechanism insight. Chemical Engineering Journal, 2020, 401, 126135.	12.7	134
42	Hydrogen production from supercritical water gasification of soda black liquor with various metal oxides. Renewable Energy, 2020, 157, 24-32.	8.9	44
43	Promotion effect of PANI on Fe-PANI/Zeolite as an active and recyclable Fenton-like catalyst under near-neutral condition. Applied Surface Science, 2020, 508, 145298.	6.1	31
44	Maleic hydrazide-based molecule doping in three-dimensional lettuce-like graphite carbon nitride towards highly efficient photocatalytic hydrogen evolution. Applied Catalysis B: Environmental, 2020, 272, 119009.	20.2	37
45	Hydrothermal Liquefaction of Polycarbonate (PC) Plastics in Sub-/Supercritical Water and Reaction Pathway Exploration. ACS Sustainable Chemistry and Engineering, 2020, 8, 7039-7050.	6.7	41
46	Simply blending Ni nanoparticles with typical photocatalysts for efficient photocatalytic H <sub>2</sub> production. Catalysis Science and Technology, 2019, 9, 7016-7022.	4.1	18
47	A self-doping strategy to improve the photoelectrochemical performance of Cu <sub>2</sub> ZnSnS <sub>4</sub> nanocrystal films for water splitting. Chemical Communications, 2019, 55, 12396-12399.	4.1	15
48	An In0.42Ga0.58N tunnel junction nanowire photocathode monolithically integrated on a nonplanar Si wafer. Nano Energy, 2019, 57, 405-413.	16.0	38
49	Effects of mixed sacrificial reagents on hydrogen evolution over typical photocatalysts. Journal of Photonics for Energy, 2019, 10, 1.	1.3	2
50	One-pot annealing preparation of Na-doped graphitic carbon nitride from melamine and organometallic sodium salt for enhanced photocatalytic H2 evolution. International Journal of Hydrogen Energy, 2018, 43, 13953-13961.	7.1	49
51	Rational construction of multiple interfaces in ternary heterostructure for efficient spatial separation and transfer of photogenerated carriers in the application of photocatalytic hydrogen evolution. Journal of Power Sources, 2018, 379, 249-260.	7.8	37
52	Rapid high-temperature treatment on graphitic carbon nitride for excellent photocatalytic H2-evolution performance. Applied Catalysis B: Environmental, 2018, 233, 80-87.	20.2	79
53	Multiple carrier-transfer pathways in a flower-like In <sub>2</sub> S <sub>3</sub> /CdIn <sub>2</sub> S <sub>4</sub> /In <sub>2</sub> O <sub>3</sub> ternary heterostructure for enhanced photocatalytic hydrogen production. Nanoscale, 2018, 10, 7860-7870.	5.6	98
54	Hydrothermal growth of Co3(OH)2(HPO4)2 nano-needles on LaTiO2N for enhanced water oxidation under visible-light irradiation. Applied Catalysis B: Environmental, 2018, 232, 268-274.	20.2	30

#	Article	IF	CITATIONS
55	Self-assembled nanohybrid of cadmium sulfide and calcium niobate: Photocatalyst with enhanced charge separation for efficient visible light induced hydrogen generation. Catalysis Today, 2018, 315, 117-125.	4.4	21
56	Localized NiS <sub>2</sub> Quantum Dots on g <sub>3</sub> N <sub>4</sub> Nanosheets for Efficient Photocatalytic Hydrogen Production from Water. ChemCatChem, 2018, 10, 5441-5448.	3.7	46
57	Molten Ag <sub>2</sub> SO <sub>4</sub> â€based Ionâ€Exchange Preparation of Ag <sub>0.5</sub> La <sub>0.5</sub> TiO <sub>3</sub> for Photocatalytic O <sub>2</sub> Evolution. Chemistry - an Asian Journal, 2017, 12, 882-889.	3.3	8
58	WO <sub>3</sub> /g-C <sub>3</sub> N <sub>4</sub> composites: one-pot preparation and enhanced photocatalytic H <sub>2</sub> production under visible-light irradiation. Nanotechnology, 2017, 28, 164002.	2.6	78
59	LaTiO2N–LaCrO3: continuous solid solutions towards enhanced photocatalytic H2 evolution under visible-light irradiation. Dalton Transactions, 2017, 46, 10685-10693.	3.3	6
60	Surface treatment effect on the photocatalytic hydrogen generation of CdS/ZnS core-shell microstructures. Chinese Journal of Catalysis, 2017, 38, 489-497.	14.0	31
61	One-pot preparation of porous Cr2O3/g-C3N4 composites towards enhanced photocatalytic H2 evolution under visible-light irradiation. International Journal of Hydrogen Energy, 2017, 42, 4651-4659.	7.1	45
62	NH3-treated MoS2 nanosheets as photocatalysts for enhanced H2 evolution under visible-light irradiation. Journal of Alloys and Compounds, 2016, 688, 368-375.	5.5	35
63	Continuous solid solutions of Na <sub>0.5</sub> La <sub>0.5</sub> TiO <sub>3</sub> –LaCrO <sub>3</sub> for photocatalytic H <sub>2</sub> evolution under visible-light irradiation. RSC Advances, 2016, 6, 51801-51806.	3.6	9
64	A comparative study on structural and electronic properties and formation energy of bulk α-Fe2O3 using first-principles calculations with different density functionals. Computational Materials Science, 2016, 113, 117-122.	3.0	15
65	Photoelectrochemical stability improvement of cuprous oxide (Cu <sub>2</sub> 0) thin films in aqueous solution. International Journal of Energy Research, 2016, 40, 112-123.	4.5	33
66	Enhanced adsorption capacity of polypyrrole/TiO <sub>2</sub> composite modified by carboxylic acid with hydroxyl group. RSC Advances, 2016, 6, 42572-42580.	3.6	15
67	PbO-sensitized ZnO nanorod arrays for enhanced visible-light-driven photoelectrochemical performance. Journal of Materials Research, 2016, 31, 1622-1630.	2.6	11
68	Co <sub>3</sub> (OH) <sub>2</sub> (HPO <sub>4</sub> ) <sub>2</sub> as a novel photocatalyst for O <sub>2</sub> evolution under visible-light irradiation. Catalysis Science and Technology, 2016, 6, 8080-8088.	4.1	27
69	Novel cubic-phase pyrochlore Sb(III)2Sn(IV)2O7 transformed from Sn(II)2Sb(V)2O7: First-principles calculation-based prediction and experimental evidence. Materials and Design, 2016, 110, 207-213.	7.0	5
70	Light-driven removal of rhodamine B over SrTiO <sub>3</sub> modified Bi <sub>2</sub> WO <sub>6</sub> composites. RSC Advances, 2016, 6, 83471-83481.	3.6	11
71	Photocatalytic hydrogen production using twinned nanocrystals and an unanchored NiSx co-catalyst. Nature Energy, 2016, 1, .	39.5	313
72	Eosin Y-sensitized nanosheet-stacked hollow-sphere TiO2 for efficient photocatalytic H2 production under visible-light irradiation. Journal of Nanoparticle Research, 2015, 17, 1.	1.9	8

#	Article	IF	CITATIONS
73	A cocatalyst-free Eosin Y-sensitized p-type of Co <sub>3</sub> O <sub>4</sub> quantum dot for highly efficient and stable visible-light-driven water reduction and hydrogen production. Physical Chemistry Chemical Physics, 2015, 17, 21397-21400.	2.8	42
74	Functionalized nanostructures for enhanced photocatalytic performance under solar light. Beilstein Journal of Nanotechnology, 2014, 5, 994-1004.	2.8	22
75	Semiconductor-Based Photocatalytic, Photoelectrochemical, and Photovoltaic Solar-Energy Conversion. Scientific World Journal, The, 2014, 2014, 1-1.	2.1	2
76	Configuration dependence of the properties of Cd <sub>1–<i>x</i></sub> <scp>Z</scp> n <sub><i>x</i></sub> <scp>S</scp> solid solutions by firstâ€principles calculations. Physica Status Solidi (B): Basic Research, 2014, 251, 655-660.	1.5	5
77	A Firstâ€Principles Investigation on Microscopic Atom Distribution and Configurationâ€Averaged Properties in Cd <sub>1â^<i>x</i></sub> Zn <sub><i>x</i></sub> S Solid Solutions. ChemPhysChem, 2014, 15, 3125-3132.	2.1	6
78	Co3O4 quantum dots: reverse micelle synthesis and visible-light-driven photocatalytic overall water splitting. Chemical Communications, 2014, 50, 2002.	4.1	89
79	Photocatalytic reforming of glucose under visible light over morphology controlled Cu <sub>2</sub> O: efficient charge separation by crystal facet engineering. Chemical Communications, 2014, 50, 192-194.	4.1	92
80	Ag3PO4 photocatalyst: Hydrothermal preparation and enhanced O2 evolution under visible-light irradiation. International Journal of Hydrogen Energy, 2013, 38, 11870-11877.	7.1	57
81	Enhanced photocatalytic hydrogen production activity of chromium doped lead niobate under visible-light irradiation. Applied Catalysis A: General, 2013, 468, 403-409.	4.3	13
82	Controllable synthesis of double layered tubular CdSe/ZnO arrays and their photoelectrochemical performance for hydrogen production. Applied Catalysis B: Environmental, 2013, 138-139, 304-310.	20.2	24
83	CdS/CdSe Core–Shell Nanorod Arrays: Energy Level Alignment and Enhanced Photoelectrochemical Performance. ACS Applied Materials & Interfaces, 2013, 5, 4021-4025.	8.0	60
84	Efficient Photocatalytic Hydrogen Evolution Under Visible Light Over a Mesoporous Titania Crystallized by Thermal Treatment in Hydrogen. Science of Advanced Materials, 2013, 5, 982-986.	0.7	4
85	Visible light-driven photocatalysis of doped SrTiO_3 tubular structure. Optics Express, 2012, 20, A351.	3.4	16
86	CaTaO2N–CaZrO3 solid solution: Band-structure engineering and visible-light-driven photocatalytic hydrogen production. International Journal of Hydrogen Energy, 2012, 37, 13704-13710.	7.1	36
87	First-principles calculations of Cd1â°'xZnxS doped with alkaline earth metals for photocatalytic hydrogen generation. International Journal of Hydrogen Energy, 2012, 37, 13074-13081.	7.1	9
88	A novel Sn2Sb2O7 nanophotocatalyst for visible-light-driven H2 evolution. Nano Research, 2012, 5, 576-583.	10.4	22
89	ABO3-based photocatalysts for water splitting. Progress in Natural Science: Materials International, 2012, 22, 592-615.	4.4	243
90	A multichannel system for rapid determination of the activity for photocatalytic H <sub>2</sub> production. AICHE Journal, 2012, 58, 3593-3596.	3.6	7

#	Article	IF	CITATIONS
91	Tin(II) Antimonates with Adjustable Compositions: Effects of Bandâ€Gaps and Nanostructures on Visibleâ€Lightâ€Driven Photocatalytic H <sub>2</sub> Evolution. ChemCatChem, 2012, 4, 1389-1396.	3.7	13
92	Siteâ€Selected Doping of Upconversion Luminescent Er <sup>3+</sup> into SrTiO <sub>3</sub> for Visibleâ€Lightâ€Driven Photocatalytic H <sub>2</sub> or O <sub>2</sub> Evolution. Chemistry - A European Journal, 2012, 18, 7543-7551.	3.3	87
93	Singleâ€Crystal Nanosheetâ€Based Hierarchical AgSbO <sub>3</sub> with Exposed {001} Facets: Topotactic Synthesis and Enhanced Photocatalytic Activity. Chemistry - A European Journal, 2012, 18, 3157-3162.	3.3	51
94	Visible-light-driven photocatalytic water splitting on nanostructured semiconducting materials. International Journal of Nanotechnology, 2011, 8, 523.	0.2	82
95	First-principles study on absolute band edge positions for Il–VI semiconductors at (110) surface. Chemical Physics Letters, 2011, 513, 72-76.	2.6	9
96	Hydrothermal Synthesis of Na <sub>0.5</sub> La <sub>0.5</sub> TiO <sub>3</sub> –LaCrO <sub>3</sub> Solidâ€Solution Singleâ€Crystal Nanocubes for Visibleâ€Lightâ€Driven Photocatalytic H <sub>2</sub> Evolution. Chemistry - A European Journal, 2011, 17, 7858-7867.	3.3	43
97	Hydrogen production under visible light by photocatalytic reforming of glucose over an oxide solid solution photocatalyst. Catalysis Communications, 2010, 12, 264-267.	3.3	34